

Geophysical Research Letters[®]

RESEARCH LETTER

10.1029/2022GL099730

Key Points:

- We analyzed Holocene temperature-precipitation correlations and hydrological sensitivities using climate proxy (pollen) and model data from Northern Hemisphere extratropics
- We found reversals to negative temperature-precipitation correlations from the cold early Holocene to the warm mid-Holocene likely related to moisture-limited convection
- Correlations and hydrological sensitivities were mostly stable positive in polar and extratropical monsoon-areas

Supporting Information:

Supporting Information may be found in the online version of this article.

Correspondence to:

U. Herzschuh,
Ulrike.Herzschuh@awi.de

Citation:

Herzschuh, U., Böhmer, T., Li, C., Cao, X., Hébert, R., Dallmeyer, A., et al. (2022). Reversals in temperature-precipitation correlations in the Northern Hemisphere extratropics during the Holocene. *Geophysical Research Letters*, 49, e2022GL099730. <https://doi.org/10.1029/2022GL099730>

Received 31 MAY 2022

Accepted 7 SEP 2022

Author Contributions:

Data curation: Chenzhi Li, Xianyong Cao
Formal analysis: Thomas Böhmer, Raphaël Hébert
Investigation: Anne Dallmeyer
Methodology: Xianyong Cao, Richard J. Telford, Stefan Kruse
Visualization: Thomas Böhmer

Reversals in Temperature-Precipitation Correlations in the Northern Hemisphere Extratropics During the Holocene

Ulrike Herzschuh^{1,2,3} , Thomas Böhmer¹ , Chenzhi Li^{1,2} , Xianyong Cao^{1,4} , Raphaël Hébert¹ , Anne Dallmeyer⁵ , Richard J. Telford⁶ , and Stefan Kruse¹ 

¹Polar Terrestrial Environmental Systems, Alfred Wegener Institute Helmholtz Centre for Polar and Marine Research, Potsdam, Germany, ²Institute of Environmental Science and Geography, University of Potsdam, Potsdam, Germany, ³Institute of Biochemistry and Biology, University of Potsdam, Potsdam, Germany, ⁴Alpine Paleocology and Human Adaptation Group (ALPHA), State Key Laboratory of Tibetan Plateau Earth System, Resources and Environment (TPESRE), Institute of Tibetan Plateau Research, Chinese Academy of Sciences, Beijing, China, ⁵Max Planck Institute for Meteorology, Hamburg, Germany, ⁶Department of Biological Sciences, University of Bergen and Bjerknes Centre for Climate Research, Bergen, Norway

Abstract Future precipitation levels remain uncertain because climate models have struggled to reproduce observed variations in temperature-precipitation correlations. Our analyses of Holocene proxy-based temperature-precipitation correlations and hydrological sensitivities from 2,237 Northern Hemisphere extratropical pollen records reveal a significant latitudinal dependence and temporal variations among the early, middle, and late Holocene. These proxy-based variations are largely consistent with patterns obtained from transient climate simulations (TraCE21k). While high latitudes and subtropical monsoon areas show mainly stable positive correlations throughout the Holocene, the mid-latitude pattern is temporally and spatially more variable. In particular, we identified a reversal from positive to negative temperature-precipitation correlations in the eastern North American and European mid-latitudes from the early to mid-Holocene that mainly related to slowed down westerlies and a switch to moisture-limited convection under a warm climate. Our palaeoevidence of past temperature-precipitation correlation shifts identifies those regions where simulating past and future precipitation levels might be particularly challenging.

Plain Language Summary Predicting future precipitation levels reliably is more challenging than predicting temperature change. Accordingly, we need to understand the relationship between temperature and precipitation and its changes in space and time. We used climate proxy-data derived from 2,237 pollen records from lake sediments and peats from the Northern Hemisphere extratropics for the early, middle, and late Holocene (i.e., 12,000–8,000, 8,000–4,000, 4,000–0 years before present, respectively). Our results reveal a significant latitudinal dependence and temporal variation of the temperature-precipitation relationship. These proxy-based variations are largely consistent with patterns obtained from simulations using climate models. While high latitudes and subtropical monsoon areas show mainly stable positive correlations throughout the Holocene (i.e., warm conditions co-occur with wet conditions), the mid-latitude pattern is temporally and spatially more variable. In particular, we identified a reversal to negative temperature-precipitation correlations in the eastern North American and European mid-latitudes from the early to middle Holocene. We hypothesize that weak westerly circulation, warm climate, and climate-soil feedbacks limited evaporation and as such reduced convection during the middle Holocene which led to a negative relationship between temperature and precipitation. Our analysis of past temperature-precipitation correlation shifts identifies regions where past changes in the temperature-precipitation relationships are variable and thus where predicting precipitation might be particularly challenging in a warming climate.

1. Introduction

Understanding changes in precipitation patterns over land areas during climatic warming is of utmost importance for the reliable prediction of climate-change impacts on terrestrial ecosystems and on human societies (Trenberth, 2011). Precipitation and temperature are interconnected through numerous physical processes that vary with both location and time (Trenberth, 2011), especially within the extratropical regions (Adler et al., 2008; Routson et al., 2019). Temperature-precipitation co-variation and its variation across the temporal scale is therefore an important aspect of climate model validation (Hao et al., 2019; Nogueira, 2019a; Wu et al., 2013). Climate

© 2022. The Authors.

This is an open access article under the terms of the [Creative Commons Attribution-NonCommercial-NoDerivs License](https://creativecommons.org/licenses/by/4.0/), which permits use and distribution in any medium, provided the original work is properly cited, the use is non-commercial and no modifications or adaptations are made.

Writing – review & editing: Chenzhi Li, Xianyong Cao, Raphaël Hébert, Anne Dallmeyer, Richard J. Telford, Stefan Kruse

models have, to date, been largely unable to reproduce recently observed changes in the relationship between precipitation and temperature (Hao et al., 2019), and future trends in both precipitation and temperature are consequently uncertain because of their interdependence.

The global hydrological cycle is generally assumed to strengthen under warmer conditions in accordance with the theoretical Clausius-Clapeyron relationship, which describes the sensitivity of precipitable water vapor to temperature variations (Allen & Ingram, 2002; Trenberth et al., 2003). Climate models simulate an increase in global precipitation at a rate of approximately 1%–3% per Kelvin of global surface warming (Rehfeld et al., 2020). It has been shown that the hydrological sensitivity depends mainly on temperature while the contributions from changes in surface radiation and ocean heat uptake are found to be secondary (Siler et al., 2019). Accordingly, the highest rate of precipitation increase per K change, that is, the strongest hydrological sensitivity, is expected at high latitudes (O’Gorman & Schneider, 2008; Siler et al., 2019) or, generally, under cold climates.

These assumptions are rooted mainly in our knowledge of hydrological responses to warming in ocean areas or at the ocean-dominated global scale, while we still lack an understanding of the major processes governing precipitation response to warming on land, particularly with respect to processes over multi-decadal and longer time-scales. The Northern Hemisphere extratropics show no correlations between monthly temperature and precipitation in most of the mid-latitudes, weak positive correlation in most Eurasian areas to the north of 60°N, and weak negative correlations in the subtropics and so contrast with the widespread positive temperature-precipitation correlations in the ocean areas (Adler et al., 2008). Spectral analyses of instrumental precipitation products revealed that at a global scale the Clausius-Clapeyron is not the single dominant mechanism governing precipitation over land; instead, various processes acting on different time-scales cause a highly complex temperature-precipitation relationship (Nogueira, 2019b). That dry areas get drier in times of warming and wet areas get wetter in times of warming (i.e., referring to negative vs. a positive temperature-precipitation relationship depending on the precipitation-to-evaporation ratio) is a commonly referred concept (Held & Soden, 2006). However, this concept could only be confirmed for about 11% of global land areas (Greve et al., 2014). So it is still under debate whether complex local climatological interactions (e.g., temperature-dependent convection) or broad-scale atmospheric circulation features (Byrne & O’Gorman, 2015; Seager et al., 2010) determine the spatial pattern of precipitation temperature-relationships (Ljungqvist et al., 2019). Alternatively, the dependency of precipitation on temperature may mainly be a matter of the time-scale over which the correlations are investigated (Nogueira, 2019b; Rehfeld & Laepple, 2016). For example, at the global scale, a weak positive correlation already exists at sub-annual time-scales, but only becomes significant at interannual to decadal time-scales. Furthermore, the period for which temperature and precipitation measurements are available might simply be too short to examine temperature-precipitation relationships as many of the relevant mechanistic feedbacks between the two variables operate over multi-decadal to millennial time-scales (Trenberth, 2011). Furthermore, the recent rapid and interdependent changes in climate drivers such as CO₂, aerosols, and solar irradiance, which are responsible for temperature and hydrological sensitivity patterns (Samset et al., 2016), make it difficult to attribute observed temperature-precipitation relationships to any one particular driver.

Climate proxy information on past co-variations of temperature and precipitation would therefore be of great value for the validation of relevant climate model outputs (Harrison et al., 2014; Ljungqvist et al., 2019). Previous broad-scale syntheses of Holocene climate proxy information have been largely restricted to temperature and have included relatively few records from the vast Asian continent which was located outside the impact of the vanishing Laurentide ice-shield (Kaufman et al., 2020; Marsicek et al., 2018). Routson et al. (2019) found that during the Holocene a weakening low-to-high temperature gradient contributed to a precipitation decline between 50° and 30°N. The spatial pattern in temperature-precipitation correlations and their variations during the Holocene, as well as their dependency on time-scale, however, remain largely unknown.

Pollen data are the only land-derived proxy data available that, in principle, could contain both temperature and precipitation information in the same record and have sufficient temporal and spatial coverage to allow temperature-precipitation correlations to be extracted (Chevalier et al., 2020).

Here we use existing datasets (Herzschuh, Böhmer, et al., 2022, Text S1 in Supporting Information S1) to calculate temperature-precipitation correlation coefficients and local hydrological sensitivities on a 500-year time-scale for the early (12–8 ka BP), middle (8–4 ka BP), and late (4–0 ka BP) Holocene and interpret the spatial and temporal patterns. We also compare the proxy-based information to correlation coefficients and hydrological sensitivity derived from precipitation and temperature estimates from TraCE21k model simulations (He, 2010),

the only available model results that transiently cover the entire Holocene with a full general atmospheric circulation (Yeager et al., 2006).

2. Materials and Methods

Details of the data set and methods can be found in Text S2 in Supporting Information S1. Our approach makes use of a dataset of past temperatures (T_{July}) and precipitation (P_{ann}) published in Herzsuh, Böhmer, et al. (2022) derived from the setup and application of a transfer function using taxonomically harmonized modern and fossil pollen datasets (Herzsuh, Li, et al., 2022). Furthermore, we use instrumental climate data (Matsuura & Willmott, 2018b) and palaeoclimate model simulations (TRACE21k, He, 2010). We calculated correlations between inferred temperature and precipitation and hydrological sensitivity (i.e., the slope of the linear regression between the global temperature and precipitation percentage relative to the youngest sample) on a 500 year time-scale.

3. Results and Discussion

3.1. Characteristics of Proxy-And Model-Derived Temperature-Precipitation Relationships

Our proxy results revealed that about one third of records in all three Holocene periods show significant ($p < 0.1$) correlations between temperature and precipitation on a 500 year time-scale (Figure S6 in Supporting Information S1). An detailed evaluation of the proxy-based temperature-precipitation relationships can be found in Text S3 in Supporting Information S1. During the early Holocene, the majority of all records are positively correlated; among the significantly correlated records this rises to 69%. This is reflected by a median Pearson correlation coefficient (including all records) of 0.26 ± 0.02 and a median local hydrological sensitivity of $10.95\% \text{ K}^{-1} \pm 1.92$ for the Northern Hemisphere extratropics (Figure 1, Tables S1 and S2 in Supporting Information S1). The medians of the proxy results are in very good agreement with the TraCE21ka simulated values of 0.29 ± 0.04 and $8.24\% \text{ K}^{-1} \pm 0.84$ respectively, restricted to identical locations. (For comparison, the simulated results for global land + ocean yielded 0.52 ± 0.01 and $6.27\% \text{ K}^{-1} \pm 0.18$, respectively).

Both model simulations and proxy data are in agreement in that the majority of significant correlation coefficients ($p < 0.1$) are negative during the middle Holocene and median correlation coefficients (proxy: -0.08 ± 0.02 , model: -0.29 ± 0.04) and local hydrological sensitivities (proxy: $-9.13\% \text{ K}^{-1} \pm 2.07$, model: $-7.74\% \text{ K}^{-1} \pm 0.95$) are negative and significantly (both $p < 0.0001$) lower than those for the early Holocene. The late-Holocene correlations and hydrological sensitivities (Figure 1) are higher overall than those for the middle Holocene but lower than those of the early Holocene both for model and proxy (proxy: -0.02 ± 0.02 , $-0.16\% \text{ K}^{-1} \pm 2.43$; model: 0.19 ± 0.03 , $2.57\% \text{ K}^{-1} \pm 0.56$).

Many similarities in the spatial patterns could be observed for proxy-derived and model-derived temperature-precipitation correlation (Figure 2). We find significant fits between proxy-derived and model-derived spatial patterns of temperature-precipitation correlations for the early Holocene ($p_{\text{adj}} < 0.05$), as well as for spatial patterns of proxy-derived and model-derived differences between the early Holocene and the middle Holocene ($p_{\text{adj}} < 0.01$; Figure 2). During the early Holocene, similarities include the positive correlations in eastern North America and Alaska, and the (weak) negative correlations along the western coast. In Europe, a data-model fit is found with respect to the positive correlations in a broad band from western to North-Eastern Europe. Agreement also exists with respect to weakly negative correlation at the European margins in southern Scandinavia, the Gibraltar area, South-Eastern Europe, and the European part of Russia, although these areas are mostly covered by only a few simulation grid-boxes. In Asia, model-data agreement exists with respect to the widespread positive correlation in the eastern part of Siberia and northern and central China while mismatches exist in eastern Siberia and central Asia.

Compared with the early Holocene dominance of positive temperature-precipitation correlations, many regions switch to negative correlations in the middle Holocene, both in the proxy data and simulations. As a result, we find a significant fit ($p_{\text{adj}} < 0.01$) between the data- and model-derived anomaly maps (Figure 2d). For example, the correlation decreases in both central Europe and eastern North America. Mismatches exist in south-eastern North America and parts of northern Asia. This originates from model-data discrepancy in the mid-Holocene correlations; particularly, the strong negative correlations in most of Eurasia are not confirmed by the pollen-derived

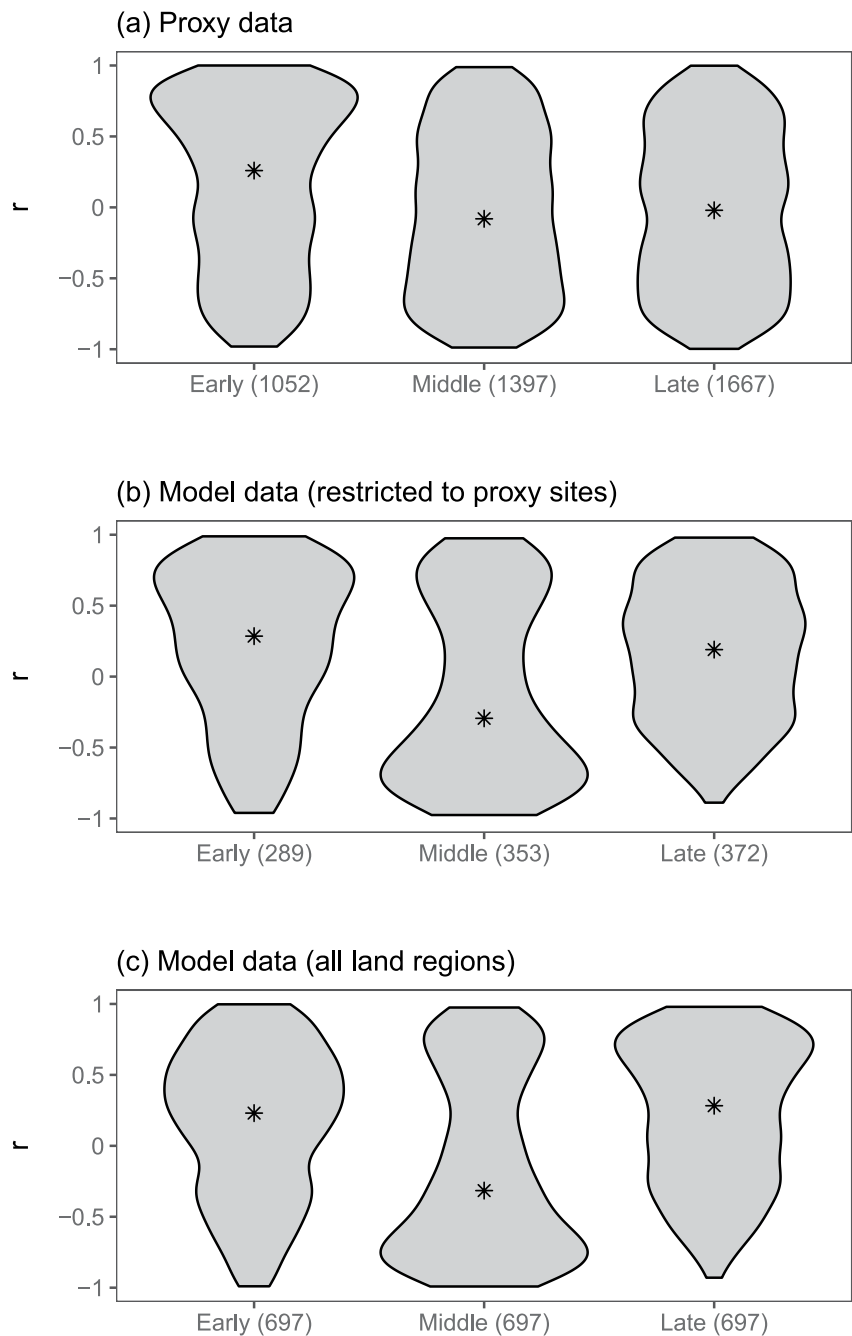


Figure 1. Distributions and medians of temperature-precipitation correlation coefficients for the Northern Hemisphere extratropics (23.5–75°N) Violin plots of temperature-precipitation correlation coefficients (r) for early (12–8 ka), middle (8–4 ka), and late (4–0 ka) Holocene pollen data (a); TraCE21k climate model simulations (restricted to proxy sites) (b), and TraCE21k climate model simulations (all northern hemisphere land regions) (c). Stars indicate median values. The shape of the proxy violin plot shows correlation results of original pollen records, while the shape of the model violin plot displays correlation results of the grid cells. (Wilcoxon test p -values for proxy data early vs. middle Holocene: <0.001 ; middle vs. late Holocene: 0.13; Wilcoxon test p -values for model simulations (restricted to early vs. middle Holocene: <0.001 ; middle vs. late Holocene: <0.001).

correlations. For the late Holocene, model-data fits exist in most of Asia and North America (but not for the north-western coast and north-eastern Canada). Pollen-derived correlations show a decline in Europe (Figure 2c), which matches with simulations, however, they are slightly negative while the data show mostly no or weakly positive correlations.

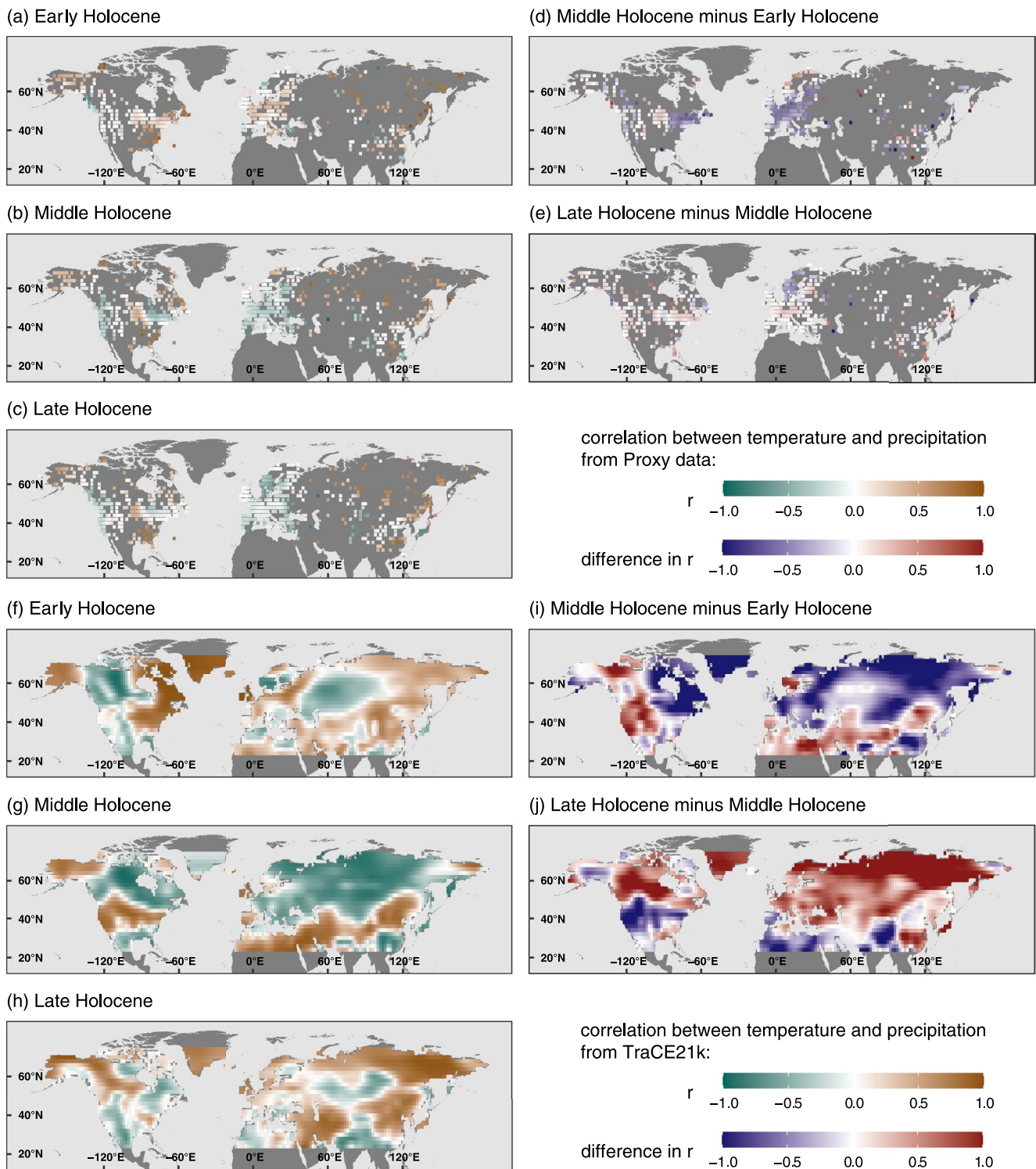


Figure 2. Temperature-precipitation correlations for the Northern Hemisphere extratropics (23.5–75°N). Upper panel: proxy data maps for (a) early Holocene, (b) middle Holocene, and (c) late Holocene and anomaly maps for middle minus (d) early Holocene and late minus (e) middle Holocene. Lower panel: TraCE21k model simulations maps for (f) early, (g) middle, and (h) late Holocene and anomaly maps for (i) middle minus early and late minus (j) middle Holocene. Figure S6 in Supporting Information S1 shows maps restricted to those proxy sites with significant correlations confirming these patterns.

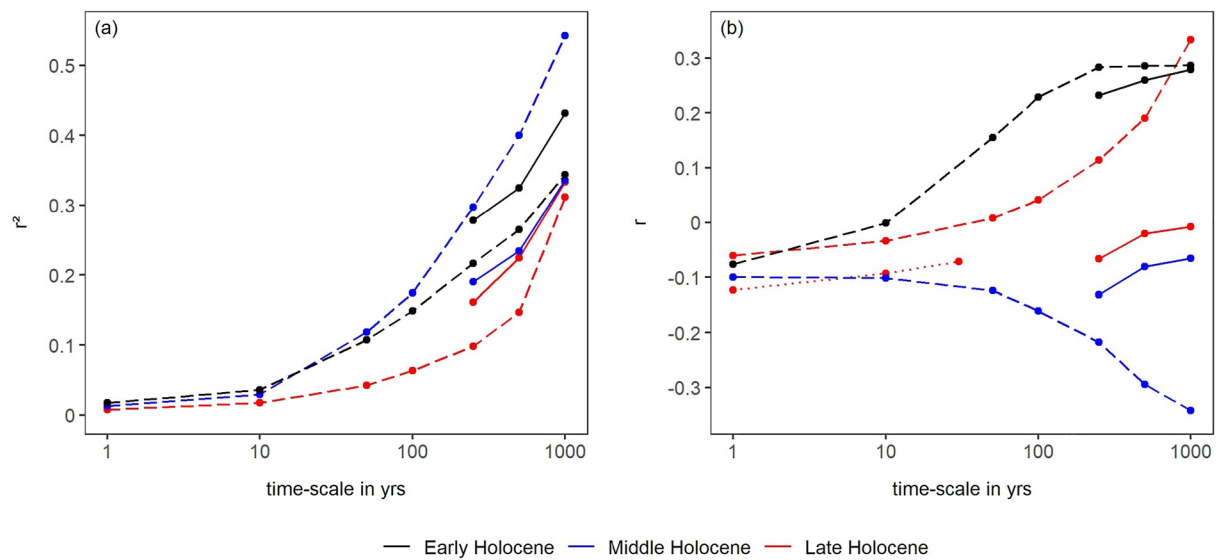


Figure 3. Temporal scaling of temperature-precipitation correlations. (a) Increasing median coefficient of determination (r^2) of temperature-precipitation correlations with time-scale for proxy (solid) and model simulations (dashed) for the early, middle, and late Holocene suggests that coherence strengthens with the time-scale used. (b) Increasing median temperature-precipitation correlation coefficient (r) with time-scale for instrumental observations (Matsuura & Willmott, 2018a, 2018b) (dotted), proxy data (solid), and model simulations (dashed) for the early, middle, and late Holocene.

We visually compared our pollen-based temperature-precipitation correlation pattern from Europe for the late Holocene on a 500 year time-scale to the decadal to centennial correlation patterns inferred from tree-ring data, which, like our data, show a gradient from a negative correlation in south-western Europe and to a positive correlation in north-eastern Europe (Ljungqvist et al., 2019).

In accordance with the Clausius-Clapeyron rule a constant hydrological sensitivity of $7\% \text{ K}^{-1}$ would be expected at global scale reflecting the theoretical precipitable water vapor sensitivity to temperature (Trenberth et al., 2003). We find that the proxy- and model-based (Table S2, Figure S7 in Supporting Information S1) median hydrological sensitivities are not equal to this constant but show marked differences between the early, middle, and late Holocene. These findings have major implications as they provide the first proxy-based indication that the Clausius-Clapeyron relationship, which forms the basis of the “wetter climate in a warmer” world assumption, is not the main factor controlling the average precipitation response to climatic warming in the Northern Hemisphere extratropical land areas over centennial to millennial time-scales. No similar analyses of temperature-precipitation correlations in proxy data have been reported to date. However, the mostly consistent trends in the medians and partly even among proxy- and model-derived spatial patterns (Figures 1 and 2, Tables S1 and S2 in Supporting Information S1) suggest that the interpreted signals originate from mechanisms that are already taken into account in the models.

We also investigated the changes of the correlation coefficient and the squared correlation coefficient (coefficient of determination) between temperature and precipitation with increase of time-scale for model simulations, instrumental data, and proxy data (Figure 3). Interestingly, model simulations and proxy data agree in that the coefficient of determination increased from the centennial to the millennial time-scale consistently for the early, middle, and late Holocene, indicating a higher signal to noise level over longer time-scales. The proxy data also show an increase in the correlation coefficient with time-scale consistently for all three periods, in agreement with the climate-station instrumental data (for annual to multi-decadal time-scale, Figure 3b). However, model simulations show variable relationships between the correlation coefficient and time-scale for the early, middle, and late Holocene.

3.2. Latitudinal Peculiarities of Temperature-Precipitation Relationships

3.2.1. Strong Positive Correlations and Hydrological Sensitivities in Polar Regions

Our results yield higher temperature-precipitation correlations and local hydrological sensitivities in the northern polar regions than in the mid-latitudes (Figure 2, Figures S7 and S8 in Supporting Information S1). Local hydrological sensitivities are particularly high ($>20\% \text{ K}^{-1}$) in northern North America and northern Asia during the early Holocene, when climate was still characterized by relatively low temperatures originating from the end of the last ice age (Figure S8 in Supporting Information S1; Routson et al., 2019). Our results provide a first proxy-based quantitative estimate of the warming effect on precipitation in cold regions on a centennial time-scale. Our finding of a particularly strong effect is consistent with concepts about high hydrological sensitivity in high northern latitudes. The proportion of solar radiation that is used for evaporation from wet land surfaces is known to depend on the background temperature, that is, it is associated with limitations on the water-holding capacity of the atmosphere (Li et al., 2013; O’Gorman & Schneider, 2008). This is because the maximum evaporative fraction increases less rapidly than the saturation vapor pressure, resulting in high sensitivities at low background temperatures (Li et al., 2013). This evaporation effect over land is enhanced when concomitant with sea-ice loss in nearby ocean areas (Bintanja & Selten, 2014). Moisture transport to the Arctic may be amplified with warming, as the stronger warming of the polar regions compared to the mid-latitudes leads to changes in the stationary wave pattern (e.g., Sang et al., 2022) This contributes to the strong hydrological sensitivity in the Arctic (Zhang et al., 2013). Controversy still exists whether or not this is in a similar order of magnitude as evaporation effects (Bintanja & Selten, 2014). Overall, the recent precipitation increase observed in and predicted for the Arctic in conjunction with warming (Trenberth, 2011) is a good analogy of our finding of high early Holocene precipitation sensitivity despite the forcing mechanisms differing. This is in line with the results of a simulation study that indicated that the processes that contribute to hydrological sensitivity are rather similar among different forcings (Stjern et al., 2019). However, there also exists contradictory evidence. For example, while simulation results of Cao et al. (2019) generally support a higher hydrological sensitivity with boundary conditions of the Last Glacial Maximum they find that the impact of the different forcings is substantial, such that the impact of the adjusted land-surface scheme is more important than the direct ice-shield impact. Furthermore, their latitudinal hydrological sensitivity gradients differ from our early Holocene results.

3.2.2. Temperature-Precipitation Correlation Switches in the Mid-Latitudes

Most of the temporal correlation sign reversals occur at mid-latitudes (Figure 2), particularly in the North American and European areas bordering the Atlantic Ocean—which are currently characterized by a humid continental climate. For example, about 50% of proxy records from around 50°N in this area switched from a positive correlation to a negative correlation between the early Holocene and the middle Holocene (Figure S9a in Supporting Information S1). This pattern is confirmed when only assessing the switches of the significantly correlated records (Figure S11 in Supporting Information S1).

We assume that the marked positive relationships between temperature and precipitation observed in the circum-North Atlantic region during the early Holocene relate to a glacially impacted climate characterized by low temperature and precipitation levels at the beginning of the early Holocene and subsequent warming and wetting (Shuman & Plank, 2011) in response to the Laurentide Ice Sheet decay. Simulations of the Last Glacial Maximum suggest that the presence of ice sheets and altered land surface distribution massively impacted the circulation (Cao et al., 2019; COHMAP, 1988). Simulations studies indicate that cold periods during the glacially impacted early Holocene were likely characterized by strong westerlies (Oster et al., 2015) which is confirmed by our finding that the strength of the July westerlies declined from the early to middle Holocene in TRACE21k (Figure S12a in Supporting Information S1, Figure 4). The intensified warming in the polar region during the middle Holocene compared to the tropics led to a reduced latitudinal temperature gradient and weakened westerly wind circulation (Figure S5 and S12a in Supporting Information S1; Routson et al., 2019). Hence, the particular warm centennials during the mid-Holocene were likely characterized by a weak moisture transport to the continents and less precipitation compared with cold early Holocene periods or moderate warm periods. Likely the reduced broad-scale (stratiform) precipitation at centennial time-scales during the mid-Holocene originate from many years characterized by the occurrence of blocking systems and concurrent summer heat waves (Figure 4), as is observed in warm years under modern conditions (Coumou et al., 2015).

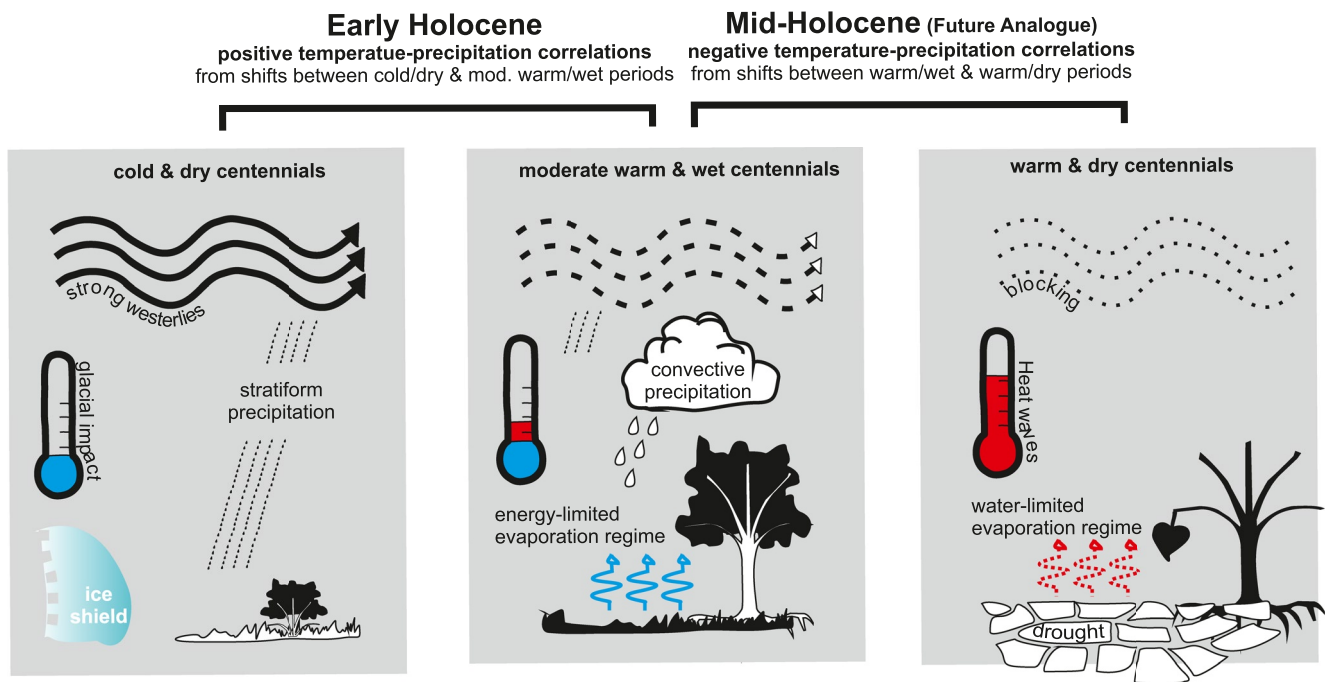


Figure 4. Sketch of the mechanisms causing the reversals in the temperature-precipitation relationships in the circum-North Atlantic sector. The early Holocene is characterized by positive temperature-precipitation correlations. Due to the impact of the Laurentide Ice Sheet the westerlies were particularly strong during cold early Holocene phases (left panel). During moderate warm early Holocene phases (middle panel), convective precipitation contributed to an overall wet climate. Negative temperature-precipitation correlations specify the mid-Holocene originating from an alternation of moderate warm and wet (middle panel) and warm and dry (right panel) centennials. The warm phases were likely characterized by many years with weak westerlies and summer blocking systems (right panel).

At present, the mid-latitudes receive only about half of their total precipitation from broad-scale atmospheric circulation systems with the balance resulting from local convective processes (Muller & O’Gorman, 2011; Seager et al., 2010). We assume that local convective conditions in particular during summer, amplified the westerlies induced early-to-mid Holocene changes (Figure 4). Early to mid-Holocene summer surface warming in the circum-North Atlantic region (Figure S8 in Supporting Information S1) led to a higher temperature difference between surface and upper atmospheric levels (Figure S12b in Supporting Information S1) and to a higher specific humidity at the surface (Figure S12c in Supporting Information S1), both strengthening convection (Figure 4; Figure S12b in Supporting Information S1). At the same time, the availability of water in soils was reduced (by up to 50% in Trace21k, Figure S12d in Supporting Information S1). In particular during warm mid-Holocene periods, reduced soil moisture likely caused a switch from an energy-limited evaporation regime to a water-limited evaporation regime during the warm season. Summer warming was likely even further amplified via soil-atmosphere feedback mechanisms (Vogel et al., 2017). Accordingly, the mid-Holocene was characterized by an alternation of moderate warm and wet (middle panel, Figure 4) and warm and dry (right panel) centennials resulting in negative temperature-precipitation relationships. The—at least regional—mid-to late-Holocene cooling (Figure S9 in Supporting Information S1) then caused, at least partly, a switch back to negative temperature-precipitation relationships (Figure 2).

This model-based conceptualisation could explain the reversal in temperature-precipitation correlation inferred from the proxy data. However, the model results reveal a strongly negative correlation during the mid-Holocene and spatially much wider changes than inferred by the reconstructions. The magnitude may be affected by the relatively coarse spatial resolution in the model, probably affecting the position of the westerly wind storm tracks (van der Linden et al., 2019). Biases in the simulated temperature and precipitation may even be enhanced by the simplified implementation of processes depicting the soil-moisture feedback. Generally, the mid-to late-Holocene changes are less obvious in the proxy data compared with the simulations and require further investigations. A better understanding of the processes governing temperature-precipitation relationships may also shed light on data-model discrepancies about temperature trends over the Holocene, called the Holocene Conundrum, which

has been attributed to variously to spatial position of proxy networks (Marsicek et al., 2018) and seasonal influences on proxy signals (Osman et al., 2021).

3.2.3. Stable Positive Correlations in Extratropical Monsoonal Areas

Most of our subtropical proxy records come from areas affected by summer monsoons. They show mainly positive temperature-precipitation correlations throughout the Holocene (Figures 1 and 2). This is consistent with previously published results (Rehfeld & Laepple, 2016) and the expectation that under a monsoonal climate, strong summer warming over the continent should result in intensified ocean-to-land moisture transport and intensified convection (Kutzbach, 1981). Our results are in accordance with spatial patterns of temperature-precipitation correlations in northern China on a decadal time-scale, which are characterized by positive/negative temperature-precipitation correlations inside/outside the area of monsoonal precipitation (Du et al., 2013). Accordingly, the shift in the main monsoonal rain band (i.e., characterized by positive temperature-precipitation correlations) from north-eastern China during the early Holocene, to northern China during the middle Holocene, and then to the Yangtze River basin during the late Holocene (Herzschuh et al., 2019), is reflected in 'anomaly maps' (Figure 2), which show a positive anomaly in correlations in the middle Holocene, when monsoonal systems were shifted northwards, and a negative anomaly in the late Holocene, when monsoonal systems retreated southward.

4. Implications and Conclusions

We investigated Holocene temperature-precipitation correlations and hydrological sensitivities from 2237 Northern Hemisphere extratropical pollen records. We observed a significant latitudinal dependence and temporal variations between the early, middle, and late Holocene. Furthermore we found that these proxy-based variations are largely consistent with patterns obtained from transient climate simulations (TraCE21k).

We observed temporal correlation sign reversals (Figure 2), particularly in the North American and European areas bordering the Atlantic Ocean from early Holocene positive correlation under cold-to-moderate warm climate to negative correlations during the moderate warm and warm mid-Holocene climate (that partly reversed during the late Holocene). We assume that at cold or moderate warm conditions during the early Holocene an energy-limited evaporation-regime occurred. While warm periods during the mid-Holocene were characterized by a moisture-limited evaporation regime. A system that at least partly reversed in the context of late Holocene cooling.

By analogy with the palaeo-evidence presented here, the Northern Hemisphere extratropics are likely to show strong, spatially heterogeneous hydrological responses to ongoing warming, partly originating from the interplay of broad-scale circulation and local convective conditions, confirming recently published observations by Chernokulsky et al. (2019). Our results imply that most polar regions get wetter in response to warming. In contrast, mid-latitude areas in central Europe and eastern North America will develop or intensify negative correlations between temperature and precipitation as years characterized by an energy-limited (Clausius-Clapeyron) relationship become more rare and years with a water-limited evaporation regime in concert with summer heat waves in response to a slow-down of the westerlies become more common. This assumption is consistent with future model projections of soil drying in western central Europe (van der Linden et al., 2019). In contrast, those previously westerly dominated areas that will in the future come under the influence of a monsoonal climate, for example, the southern part of the Russian Far East (Chernokulsky et al., 2019), may switch to positive temperature-precipitation correlations.

Our time-scale dependent analyses of correlations indicate that these interdependencies are likely to be amplified over longer time-scales. Our results therefore indicate that temperature-precipitation relationships derived from instrumental data should not be used to predict long-term responses of precipitation to temperature change. However, the proxy-inferred mid-Holocene warm period may, at least to some extent, be taken as an analogue of the long-term present and future climate though further assessments are needed whether the latitudinal patterns of hydrological sensitivities are identical between CO₂-forced warming and insolation-forced warming (Samset et al., 2018).

Conflict of Interest

The authors declare no conflicts of interest relevant to this study.

Data Availability Statement

All pollen-based reconstructions are stored at Pangaea repository <https://doi.pangaea.de/10.1594/PANGAEA.930512> (Herzschuh, Li, et al., 2022) and the R code to run the reconstructions is available at Zenodo (<https://doi.org/10.5281/zenodo.5910989>). Final results of temperature-precipitation correlations and R code for correlation and sensitivity analyses is available at Zenodo (<https://zenodo.org/record/7038402%23.YxBLIuzP3V8>).

Acknowledgments

The majority of the original pollen data were obtained from the Neotoma Paleocology Database (<https://www.neotomadb.org/>, last access: July 2020). The work of data contributors, data stewards, and the Neotoma community is gratefully acknowledged. We would like to express our gratitude to all the palynologists and geologists who, either directly or indirectly, contributed pollen data and chronologies to the dataset. We acknowledge Feng He for opening TraCE21K and Cathy Jenks for language editing. We also thank the editor and two reviewers for their constructive suggestions. This research has been supported by the European Research Council, H2020 European Research Council (GlacialLegacy; Grant No. 772852 to Ulrike Herzschuh), the Bundesministerium für Bildung und Forschung (PALMOD initiative, Grant No. 01LP1510C to Ulrike Herzschuh), and the China Scholarship Council (Grant No. 201908130165 to Chenzhi Li). Open Access funding enabled and organized by Projekt DEAL.

References

- Adler, R. F., Gu, G., Wang, J.-J., Huffman, G. J., Curtis, S., & Bolvin, D. (2008). Relationships between global precipitation and surface temperature on interannual and longer timescales (1979–2006). *Journal of Geophysical Research*, *113*(D22), D22104. <https://doi.org/10.1029/2008JD010536>
- Allen, M. R., & Ingram, W. J. (2002). Constraints on future changes in climate and the hydrologic cycle. *Nature*, *419*(6903), 228–232. <https://doi.org/10.1038/nature01092>
- Bintanja, R., & Selten, F. M. (2014). Future increases in Arctic precipitation linked to local evaporation and sea-ice retreat. *Nature*, *509*(7501), 479–482. <https://doi.org/10.1038/nature13259>
- Byrne, M. P., & O’Gorman, P. A. (2015). The response of precipitation minus evapotranspiration to climate warming: Why the “wet-get-wetter, dry-get-drier” scaling does not hold over land. *Journal of Climate*, *28*(20), 8078–8092. <https://doi.org/10.1175/JCLI-D-15-0369.1>
- Cao, J., Wang, B., & Liu, J. (2019). Attribution of the last glacial maximum climate formation. *Climate Dynamics*, *53*(3), 1661–1679. <https://doi.org/10.1007/s00382-019-04711-6>
- Chernokulsky, A., Kozlov, F., Zolina, O., Bulygina, O., Mokhov, I. I., & Semenov, V. A. (2019). Observed changes in convective and stratiform precipitation in Northern Eurasia over the last five decades. *Environmental Research Letters*, *14*(4), 045001. <https://doi.org/10.1088/1748-9326/aafb82>
- Chevalier, M., Davis, B. A. S., Heiri, O., Seppä, H., Chase, B. M., Gajewski, K., et al. (2020). Pollen-based climate reconstruction techniques for late Quaternary studies. *Earth-Science Reviews*, *210*, 103384. <https://doi.org/10.1016/j.earscirev.2020.103384>
- Climate of the Past, *7*(4), 1139–1148. <https://doi.org/10.5194/cp-7-1139-2011>
- COHMAP Members. (1988). Climatic changes of the last 18,000 years: Observations and model simulations. *Science*, *241*(4869), 1043–1052. <https://doi.org/10.1126/science.241.4869.1043>
- Coumou, D., Lehmann, J., & Beckmann, J. (2015). The weakening summer circulation in the Northern Hemisphere mid-latitudes. *Science*, *348*(6232), 324–327. <https://doi.org/10.1126/science.1261768>
- Du, H., Wu, Z., Jin, Y., Zong, S., & Meng, X. (2013). Quantitative relationships between precipitation and temperature over Northeast China, 1961–2010. *Theoretical and Applied Climatology*, *113*(3), 659–670. <https://doi.org/10.1007/s00704-012-0815-7>
- Greve, P., Orlowsky, B., Mueller, B., Sheffield, J., Reichstein, M., & Seneviratne, S. I. (2014). Global assessment of trends in wetting and drying over land. *Nature Geoscience*, *7*(10), 716–721. <https://doi.org/10.1038/ngeo2247>
- Hao, Z., Phillips, T. J., Hao, F., & Wu, X. (2019). Changes in the dependence between global precipitation and temperature from observations and model simulations. *International Journal of Climatology*, *39*(12), 4895–4906. <https://doi.org/10.1002/joc.6111>
- Harrison, S. P., Bartlein, P. J., Brewer, S., Prentice, I. C., Boyd, M., Hessler, I., et al. (2014). Climate model benchmarking with glacial and mid-Holocene climates. *Climate Dynamics*, *43*(3), 671–688. <https://doi.org/10.1007/s00382-013-1922-6>
- He, F. (2010). *Simulating transient climate evolution of the last deglaciation with CCSM 3* (Ph.D. thesis). University of Wisconsin-Madison.
- Held, I. M., & Soden, B. J. (2006). Robust responses of the hydrological cycle to global warming. *Journal of Climate*, *19*(21), 5686–5699. <https://doi.org/10.1175/JCLI3990.1>
- Herzschuh, U., Böhmer, T., Li, C., Chevalier, M., Dallmeyer, A., Cao, X., et al. (2022). LegacyClimate 1.0: A dataset of pollen-based climate reconstructions from 2594 Northern Hemisphere sites covering the late quaternary. *Earth System Science Data*, 1–29. <https://doi.org/10.5194/essd-2022-38>
- Herzschuh, U., Cao, X., Laepple, T., Dallmeyer, A., Telford, R. J., Ni, J., et al. (2019). Position and orientation of the westerly jet determined Holocene rainfall patterns in China. *Nature Communications*, *10*(1), 2376. <https://doi.org/10.1038/s41467-019-09866-8>
- Herzschuh, U., Li, C., Böhmer, T., Postl, A. K., Heim, B., Andreev, A. A., et al. (2022). LegacyPollen 1.0: A taxonomically harmonized global late quaternary pollen dataset of 2831 records with standardized chronologies. *Earth System Science Data*, *14*(7), 1–25. <https://doi.org/10.5194/essd-2022-37>
- Kaufman, D., McKay, N., Routson, C., Erb, M., Datwyler, C., Sommer, P. S., et al. (2020). A global database of Holocene paleotemperature records. *Scientific Data*, *7*(1), 115. <https://doi.org/10.1038/s41597-020-0530-7>
- Kutzbach, J. E. (1981). Monsoon climate of the early Holocene: Climate experiment with the earth’s orbital parameters for 9,000 Years ago. *Science*, *214*(4516), 59–61. <https://doi.org/10.1126/science.214.4516.59>
- Li, G., Harrison, S. P., Bartlein, P. J., Izumi, K., & Prentice, I. C. (2013). Precipitation scaling with temperature in warm and cold climates: An analysis of CMIP5 simulations. *Geophysical Research Letters*, *40*(15), 4018–4024. <https://doi.org/10.1002/grl.50730>
- Liu, Z., Zhu, J., Rosenthal, Y., Zhang, X., Otto-Bliessner, B. L., Timmermann, A., et al. (2014). The Holocene temperature conundrum. *PNAS*, *111*, E3501–E3505. <https://doi.org/10.1073/pnas.1407229111>
- Ljungqvist, F. C., Seim, A., Krusic, P. J., González-Rouco, J. F., Werner, J. P., Cook, E. R., et al. (2019). European warm-season temperature and hydroclimate since 850 CE. *Environmental Research Letters*, *14*(8), 084015. <https://doi.org/10.1088/1748-9326/ab2c7e>
- Marsicek, J., Shuman, B. N., Bartlein, P. J., Shafer, S. L., & Brewer, S. (2018). Reconciling divergent trends and millennial variations in Holocene temperatures. *Nature*, *554*(7690), 92–96. <https://doi.org/10.1038/nature25464>
- Matsuura, K., & Willmott, C. J. (2018a). Terrestrial air temperature: 1900–2017 gridded monthly time series (V 5.01). Retrieved from <http://climate.geog.udel.edu/%7Eclimate/html%5Fpages/download.html%23T2017>
- Matsuura, K., & Willmott, C. J. (2018b). Terrestrial precipitation: 1900–2017 gridded monthly time series (V 5.01). Retrieved from <http://climate.geog.udel.edu/%7Eclimate/html%5Fpages/download.html%23T2017>
- Muller, C. J., & O’Gorman, P. A. (2011). An energetic perspective on the regional response of precipitation to climate change. *Nature Climate Change*, *1*(5), 266–271. <https://doi.org/10.1038/nclimate1169>
- Nogueira, M. (2019a). The multi-scale structure of atmospheric energetic constraints on globally averaged precipitation. *Earth System Dynamics*, *10*(2), 219–232. <https://doi.org/10.5194/esd-10-219-2019>

- Nogueira, M. (2019b). The sensitivity of the atmospheric branch of the global water cycle to temperature fluctuations at synoptic to decadal time-scales in different satellite- and model-based products. *Climate Dynamics*, 52(1), 617–636. <https://doi.org/10.1007/s00382-018-4153-z>
- Nychka, M. D. (2021). Fields: Tools for spatial data (version 13.3). Retrieved from <https://CRAN.R-project.org/package=fields>
- O’Gorman, P. A., & Schneider, T. (2008). The hydrological cycle over a wide range of climates simulated with an idealized GCM. *Journal of Climate*, 21(15), 3815–3832. <https://doi.org/10.1175/2007JCLI2065.1>
- Osman, M. B., Tierney, J. E., Zhu, J., Tardif, R., Hakim, G. J., King, J., & Poulsen, C. J. (2021). Globally resolved surface temperatures since the last glacial maximum. *Nature*, 599(7884), 239–244. <https://doi.org/10.1038/s41586-021-03984-4>
- Oster, J. L., Ibarra, D. E., Winnick, M. J., & Maher, K. (2015). Steering of westerly storms over Western North America at the last glacial maximum. *Nature Geoscience*, 8(3), 201–205. <https://doi.org/10.1038/ngeo2365>
- Rehfeld, K., Hébert, R., Lora, J. M., Lofverstrom, M., & Brierley, C. M. (2020). Variability of surface climate in simulations of past and future. *Earth System Dynamics*, 11(2), 447–468. <https://doi.org/10.5194/esd-11-447-2020>
- Rehfeld, K., & Laepple, T. (2016). Warmer and wetter or warmer and dryer? Observed versus simulated covariability of Holocene temperature and rainfall in Asia. *Earth and Planetary Science Letters*, 436, 1–9. <https://doi.org/10.1016/j.epsl.2015.12.020>
- Routson, C. C., McKay, N. P., Kaufman, D. S., Erb, M. P., Goosse, H., Shuman, B. N., et al. (2019). Mid-latitude net precipitation decreased with Arctic warming during the Holocene. *Nature*, 568(7750), 83–87. <https://doi.org/10.1038/s41586-019-1060-3>
- Samset, B. H., Myhre, G., Forster, P. M., Hodnebrog, Ø., Andrews, T., Boucher, O., et al. (2018). Weak hydrological sensitivity to temperature change over land, independent of climate forcing. *Npj Climate and Atmospheric Science*, 1(1), 1–8. <https://doi.org/10.1038/s41612-017-0005-5>
- Samset, B. H., Myhre, G., Forster, P. M., Hodnebrog, Ø., Andrews, T., Faluvegi, G., et al. (2016). Fast and slow precipitation responses to individual climate forcings: A PDRMIP multimodel study. *Geophysical Research Letters*, 43(6), 2782–2791. <https://doi.org/10.1002/2016GL068064>
- Sang, X., Yang, X.-Q., Tao, L., Fang, J., & Sun, X. (2022). Decadal changes of wintertime poleward heat and moisture transport associated with the amplified Arctic warming. *Climate Dynamics*, 58(1), 137–159. <https://doi.org/10.1007/s00382-021-05894-7>
- Seager, R., Naik, N., & Vecchi, G. A. (2010). Thermodynamic and dynamic mechanisms for large-scale changes in the hydrological cycle in response to global warming. *Journal of Climate*, 23(17), 4651–4668. <https://doi.org/10.1175/2010JCLI3655.1>
- Shuman, B., & Plank, C. (2011). Orbital, ice sheet, and possible solar controls on Holocene moisture trends in the North Atlantic drainage basin. *Geology*, 39(2), 151–154. <https://doi.org/10.1130/G31387.1>
- Siler, N., Roe, G. H., Armour, K. C., & Feldl, N. (2019). Revisiting the surface-energy-flux perspective on the sensitivity of global precipitation to climate change. *Climate Dynamics*, 52(7), 3983–3995. <https://doi.org/10.1007/s00382-018-4359-0>
- Stjern, C. W., Lund, M. T., Samset, B. H., Myhre, G., Forster, P. M., Andrews, T., et al. (2019). Arctic amplification response to individual climate drivers. *Journal of Geophysical Research: Atmospheres*, 124(13), 6698–6717. <https://doi.org/10.1029/2018jd029726>
- Trenberth, K. E. (2011). Changes in precipitation with climate change. *Climate Research*, 47(1–2), 123–138. <https://doi.org/10.3354/cr00953>
- Trenberth, K. E., Dai, A., Rasmussen, R. M., & Parsons, D. B. (2003). The changing character of precipitation. *Bulletin of the American Meteorological Society*, 84(9), 1205–1218. <https://doi.org/10.1175/BAMS-84-9-1205>
- van der Linden, E. C., Haarsma, R. J., & van der Schrier, G. (2019). Impact of climate model resolution on soil moisture projections in central-Western Europe. *Hydrology and Earth System Sciences*, 23(1), 191–206. <https://doi.org/10.5194/hess-23-191-2019>
- Vogel, M. M., Orth, R., Cheruy, F., Hagemann, S., Lorenz, R., van den Hurk, B. J. J. M., & Seneviratne, S. I. (2017). Regional amplification of projected changes in extreme temperatures strongly controlled by soil moisture-temperature feedbacks. *Geophysical Research Letters*, 44(3), 1511–1519. <https://doi.org/10.1002/2016GL071235>
- Wu, R., Chen, J., & Wen, Z. (2013). Precipitation-surface temperature relationship in the IPCC CMIP5 models. *Advances in Atmospheric Sciences*, 30(3), 766–778. <https://doi.org/10.1007/s00376-012-2130-8>
- Yeager, S. G., Shields, C. A., Large, W. G., & Hack, J. J. (2006). The low-resolution CCSM3. *Journal of Climate*, 19(11), 2545–2566. <https://doi.org/10.1175/JCLI3744.1>
- Zhang, X., He, J., Zhang, J., Polyakov, I., Gerdes, R., Inoue, J., & Wu, P. (2013). Enhanced poleward moisture transport and amplified northern high-latitude wetting trend. *Nature Climate Change*, 3(1), 47–51. <https://doi.org/10.1038/nclimate1631>